Induction of Th1 and Th2 in the protection against SARS-CoV-2 through mucosal delivery of an adenovirus vaccine expressing an engineered spike protein

Nai-Hsiang Chung [a,b,c], Ying-Chin Chen [a], Shiu-Ju Yang [a], Yu-Ching Lin [a], Horng-Yunn Dou [a], Lily Hui-Ching Wang [c], Ching-Len Liao [a], Yen-Hung Chow [a,d,*]

[a] National Institute of Infectious Disease and Vaccinology, National Health Research Institutes, Zhunan, Taiwan
[b] Graduate Program of Biotechnology in Medicine, National Tsing Hua University, Hsinchu, Taiwan
[c] Institute of Molecular and Cellular Biology, National Tsing Hua University, Hsinchu, Taiwan
[d] Graduate Institute of Biomedical Sciences, China Medical University, Taichung, Taiwan

ARTICLE INFO

ABSTRACT

A series of recombinant human type 5 adenoviruses that express the full-length or membrane-truncated spike protein (S) of SARS-CoV-2 (AdCoV2-S or AdCoV2-SdTM, respectively) was tested the efficacy against SARS-CoV-2 *via* intranasal (i.n.) or subcutaneous (s.c.) immunization in a rodent model. Mucosal delivery of adenovirus (Ad) vaccines could induce anti-SARS-CoV-2 IgG and IgA in the serum and in the mucosal, respectively as indicated by vaginal wash (vw) and bronchoalveolar lavage fluid (BALF). Serum anti-SARS-CoV-2 IgG but not IgA in the vw and BALF was induced by AdCoV2-S s.c.. Administration of AdCoV2-S i.n. was able to induce higher anti-SARS-CoV-2 binding and neutralizing antibody levels than s.c. injection. AdCoV2-SdTM i.n. induced a lower antibody responses than AdCoV2-S i.n.. Induced anti-S antibody responses by AdCoV2-S via i.n. or s.c. were not influenced by the pre-existing serum anti-Ad antibody. Novelty, S-specific IgG1 which represented Th2-mediated humoral response was dominantly induced in Ad i.n.-immunized serum in contrast to more IgG2a which represented Th1-mediated cellular response found in Ad s.c.-immunized serum. The activation of S-specific IFN-γ and IL-4 in splenic Th1 and Th2 cells, respectively, was observed in the AdCoV2-S i.n. and s.c. groups, indicating the Th1 and Th2 immunity were activated. AdCoV2-S and AdCoV2-SdTM significantly prevented body weight loss and reduced pulmonary viral loads in hamsters. A reduction in inflammation in the lungs was observed in AdCoV-S via i.n. or s.c.-immunized hamsters following a SARS-CoV-2 challenge. It correlated to Th1 cytokine but no inflammatory cytokines secretions found in AdCoV-S i.n. -immunized BALF. These results indicate that intranasal delivery of AdCoV2-S vaccines is safe and potent at preventing SARS-CoV-2 infections.

© 2021 Elsevier Ltd. All rights reserved.

1. Introduction

COVID-19 is an emerging respiratory infectious disease that is caused by severe acute respiratory syndrome coronavirus 2 (SARS-CoV-2). SARS-CoV-2 is efficiently transmitted from person to person and has thus been able to spread rapidly across all continents globally.

The coronavirus is an enveloped virus containing a positive single-stranded RNA associated with a lipid membrane derived from the host cell. The coronavirus has the largest RNA genome among all the known RNA viruses [1]. Coronavirus encodes the spike (S) protein, which forms homotrimers that protrude from the surface of viral particles and is used for entry into host cells [2]. During viral replication in the infected cell, translated premature S protein is cleaved at the boundary between the S1 and S2 subunits, which remain noncovalently bound in the prefusion conformation [3]. S1 is responsible for binding to the host cell receptor, and S2 is responsible for the fusion of the viral and cellular membranes after S1–receptor interactions occur [3,4]. Recent studies have indicated that SARS-related coronaviruses, including SARS-CoV-2, interact directly with angiotensin-converting enzyme 2 (ACE2) *via* S1 to enter target cells [5].

A replication-incompetent adenoviral vector (Ad) with a recombinant E1-deficient Ad carrying a transgene has been shown to be a

potential vaccine vector in multiple successful preclinical and clinical studies [6–8]. Ad is a strong dendritic cells (DCs) activator that can coordinate and stimulate T helper (Th) cells to activate B cells for antibody secretion [9] or to trigger cellular immunity [8,10]. Distinct subsets of Th cells, such as Th1 and Th2, can be determined by what cytokines secretion upon activation [11]. In which Th1 cells produce IL-2, IFN-γ, and TNF-β, and Th2 cells produce IL-4, IL-5, IL-6, IL-10, and IL-13. The balance of cytokines produced by these subsets of Th is a key factor to skew the character of an immune response [12–14]. Th1 cells promotes cell-mediated immune responses and is required for host defense against intracellular viral and bacterial pathogens. Th2 cells mediate the activation and maintenance of the antibody-mediated immune response against extracellular parasites, bacteria, allergens, and toxins [15]. A third subset of Th cells, Th17, which secrets IL-17 have a pro-inflammatory bias. Th17 plays a key role in the defense against extracellular pathogens as well as the development of autoimmune diseases. The secretion of IL-23 from antigen-presenting cells such as DCs, which have been activated by the uptake and processing of pathogens, in turn activates Th17 cells [16]. Also, a specialized subset of CD4 T cells named T follicular helper (Tfh) cells that participating in the generation of effective and long-lived humoral immune responses to antigen [17] are required for helping antigen-specific B cells to generate the matured antibodies occurred in the germinal center [17,18]. The germinal center is the origin of long-lived memory B cells and plasma cells that populate the periphery and bone marrow (respectively), and provide long-term antibody-mediated protection against pathogens[19]. Previous studies have shown that the induction of neutralizing antibodies, as well as pathogen-specific cellular immunity against coronavirus infection, are important for effective vaccine development [20].

The Ad vector can be delivered by different routes such as systemic or mucosal site administration, which makes vaccines convenient for immunization against respiratory pathogens that preferentially initiate infection at a mucosal site or in the respiratory tract [6,8,21]. Several Ad vector-based vaccines encoding S of SARS-CoV2 had been developed and were permitted to systemic inject into people via one or two doses in clinical trials [22]. Their efficacy and safety requirement are satisfied and are proven to use in control of SARS-CoV2 infection in many countries. Chimpanzee Ad (ChAd) and human serotype 26 of Ad (Ad26) carrying of SARS-CoV2 S gene are currently used in clinic. The study of ChAd-SARS-CoV-2-S pointed out that intranasal (i.n.) injection could trigger better mucosal immune responses and inhibit SARS-CoV2 infection in human ACE2-transgenic mice [23] and in rhesus macaques [24]. Other studies showed that the Ad vaccine using the i.n. route can effectively protect some viral infections such as Ebola Zaire and respiratory syncytia virus (RSV)[25,26]. Also, i.n. immunization can effectively reduce the impact of pre-existing anti-adenovirus immunity and effectively induce an anti-pathogen immune response [25]. The approach to Ad vaccine *via* mucosal immunization is one of the application trials in the future. Other major vaccine design such as mRNA-based vaccines [27,28] also has been shown to elicit a good efficacy in preventing viral transmission. However, mRNA-based vaccines require extremely cold condition (>-20 °C) for storage and transportation that presents a challenge in clinical use, particularly for developing regions. In contrast, Ad vaccines are shown to be stable at cool condition (2–8 °C).

Here, we characterize the immunogenicity of recombinant Ad expressing S and S-engineered proteins of SARS-CoV-2 in animals. The immune responses induced by Ad vaccine mucosal immunization indicated significant Th1/Th2-balanced immunity and a reduction in pulmonary viral loads and the associated inflammation induced by SARS-CoV-2 infection. The increased efficacy of the Ad vaccine against SARS-CoV-2 when administered intranasally rather than systemically was investigated. These results support the future development of mucosal Ad vaccines for clinical use to control SARS-CoV-2.

2. Materials and methods

2.1. Ethics statement

The study was carried out in compliance with the ARRIVE guidelines. All animal experiments were conducted in accordance with the guidelines of the Laboratory Animal Center of the National Health Research Institutes (LAC-NHRI) in Taiwan. The animal use protocols were reviewed and approved by the NHRI Institutional Animal Care and Use Committee (Approval Protocol No. NHRI-IACUC-109073-M1-A-S01). To perform immunization or a viral challenge, the animals were placed in an anesthetic inhalator inhalation chamber containing isoflurane (initial phase: 5%; maintenance phase: 3%–4%) for 1 min before vaccine administration or SARS-CoV-2 challenge. After the investigation, the animals were euthanized by 100% CO_2 inhalation for 5 min followed by cervical dislocation to minimize suffering.

2.2. Cell lines and viruses

Human embryonic kidney cells (293A) were purchased from Invitrogen (Cat. R70507), and green monkey kidney cells (Vero) were purchased from the American Type Culture Collection (ATCC No. CCL-81). The 293 cells were cultured, grown and maintained in DMEM (HyClone, Cat. SH300) supplemented with 10% FBS in an incubator at 37 °C with 5% CO_2. Vero cells were cultured, grown and maintained in M199 medium (GIBCO-BRL) supplemented with 5% FBS in an incubator at 37 °C with 5% CO_2. The SARS-CoV-2 strain (hCoV-19/Taiwan/4/2020) was isolated from the Taiwan Centers for Disease Control and propagated in Vero cells. The propagation of SARS-CoV-2 was performed in the P3-grade laboratory, which was maintained in accordance with the regulations and approved by the Taiwan CDC inspection service. The viral stocks were stored at –80 °C. Viral stock titers were tested by cytopathic effect (CPE), and the $TCID_{50}$ values were calculated by Reed-Muench method.

2.3. Animals, immunization, and live SARS-CoV2 challenge

BALB/c mice and Syrian hamsters (purchased from the National Laboratory Animal Center, Taiwan) aged six to ten weeks were maintained in pathogen-free cages at the LAC-NHRI throughout the animal study. The BALB/c mice were primed with 1×10^7 pfu/50 μl of Ad intranasally (i.n.) or subcutaneously (s.c.). After 14 days, the mice were boosted with the same dose of the respective immunogens administered *via* the same route. The mice were bled at 14 days and 1, 2, and 3 months after the booster immunization. The serum was analyzed by ELISA for the binding activity to recombinant S expressed in Sf9 insect cells (GenScript, Cat. Z0.481–100) and for neutralizing activity against SARS-CoV-2 by the neutralization- $TCID_{50}$ assay. For the challenge studies performed in the P3 laboratory, 1×10^5 $TCID_{50}$/hamster of live SARS-CoV-2 was administered i.n. 1 month after the second immunization. The hamsters were monitored for 6 days to record their body weights or sacrificed on days 3 and 6 after viral challenge, and the lung tissues were isolated for plaque assays and histochemistry.

Whole lungs were excised from the hamsters and homogenized, clarified, and titrated by the $TCID_{50}$ on Vero cells in 96-well plates. The cells were inoculated with serially diluted lung homogenate in M199 with 5% FBS and incubated for 5 days. The cells were visual-

ized when 50% were lysed by microscopy and used as sets of diluted lung homogenates according to the calculation of the virus titer in the sample.

For histochemistry, the lung tissues were placed directly into 10% formalin (Sigma-Aldrich) solution overnight and embedded in paraffin for sectioning. The sections were stained with 1% H/E, and the pictures of each section were obtained at 100× and 200× magnification (Nikon DXM1200 CCD digital camera). The severity of inflammation in the H/E-stained sections was scored by following the reported criteria: grade 1: mixed mononuclear cell infiltrate next to the bronchus; grade 2: diffuse monocyte infiltration in alveolar spaces; grade 3: mixed diffuse infiltrates and small foci of mixed mononuclear cells (BALT); and grade 4: extensive dense collections of BALT and diffuse infiltrates [29].

2.4. Production of recombinant Ads

E1 and E3 genes-deleted recombinant human adenovirus type 5-based vector was used to construct and produce AdCoV2 vaccines. AdCoV2 which encodes the codon-optimized SARS-CoV-2′s S (AdCoV2-S) gene and transmembrane-deleted S (AdCoV2-SdTM) gene, the mutant S (AdCoV2-S(GA)) gene that has 2 amino acids mutated from LY to GA at 611 and 612 residues of S, and the codon-optimized S gene of SARS-CoV (AdSARS-S), were cloned and generated with the pAd⁄CMV⁄V5-DEST™ Gateway Vector Kit (purchased from Cat. V49320, ThermoFisher Scientific) [30,31]. AdCoV2-S(GA) and AdSARS-S that are not related to this study are only shown in the supplementary Fig. 1. Ad-LacZ, which encodes the reporter gene bacterial β-galactosidase (LacZ), was also constructed as a control vector. The propagation of AdCoV2-S, AdCoV2-SdTM, and Ad-LacZ was performed in adherent 293A cells in the presence of 10% FBS [6]. Three days after Ad infection, cell pellets were harvested for freezing and thawing twice at –80 °C for 30 min and 37 °C for 1 min. The lysates were centrifuged at 3500 rpm for 15 min at room temperature (RT), and the supernatants that contained Ad were collected. Recombinant Ad was purified and concentrated using Vivapure adenoPACK 100RT (Satorius Stedin Biotech). The purified viral titer was determined using a modified standard plaque assay [6].

2.5. Western blot

Parts of the culture medium and the lysate were harvested from the Ad-infected or non-infected 293cells. Lysates were extracted to obtain cytosolic and membrane fractions by using Mem-PER Plus Membrane Protein Extraction Kit (ThermoFisher Scientific, Cat. 89842). Ten micrograms of cytosolic and membrane fractions was individually mixed with loading dye, heated in a boil water for 3 min, and loaded onto each well in a 10% SDS-polyacrylamide gel (SDS-PAGE; Amersham Biosciences-GE Healthcare, USA) and subjected to electrophoresis in 1× Tris-glycine SDS-running buffer (pH 8.3). 20 µg Mab5 (20 µg/sample, a monoclonal antibody produced from a hybridoma line which was derived from the recombinant SARS's S protein-immunized BALB/c mouse's spleen) was mixed with 20 µl Protein G PLUS-Agarose (Santa Cruz, Cat. sc-2002) and then supplemented with 1× PBS (pH 7.0) to 300 µl following slow end-over-end mixing for 1 h at RT. 1 mL culture medium sample were centrifuged at 12,000g for 10 min and then the supernatant was went through a 100 K MWCO cutoff tube to collect 300 µl of the residual supernatant. The Mab5-Protein G complexes were mixed with the concentrated supernatant and incubated on slow end-over-end mixing for overnight at 4 °C. The precipitates were span at 1000g for 3 min and the pellets were washed three times with 1× PBS (pH 7.0). The precipitates were ready to mix with loading dye for following 10% SDS-polyacrylamide gel electrophoresis as described above. The SDS-

PAGE gel was resolved, and the proteins in the gel were then transferred onto a nitrocellulose membrane (Hybond-ECL, Amersham Biosciences-GE Healthcare, USA). The membrane was soaked in 5% skim milk in 1× PBS buffer (pH 7.0) for 1 h at RT and then incubated with diluted SARS spike protein antibody, Mab5 (1:5000) for detecting antigens derived from the cytosolic and membrane fractions, or SARS-CoV-2 (COVID-19, 2019-nCoV) spike antibody (1:3000; ProSci, Cat. 3525) for IP samples, or anti-S antibody (1:12,000, TaiVax, Cat. TVX-IRP001) for samples from the vaccine immunized serum or vw. The membrane stained with beta-actin antibody (1:10,000; Novus, Cat. NB600-501) or ATP1A1 monoclonal antibody (1:2000; Abnova, Cat. MAB2407) as internal controls for cytosolic or membrane fractions, respectively, for 14 to 16 h at 4 °C. The membrane was subsequently washed with 1× PBS plus 0.05% Tween 20 (PBS-T) followed by incubation with the respective antibodies conjugated with HRP, anti-mouse IgG antibody (1:10,000; ThermoFisher Scientific, Cat. 31430) or anti-rabbit antibody (1:10,000; Genetex, Cat. GTX213110-01), respectively. After 1 h of incubation, the membrane was washed three times with PBS-T, the Millipore ECL substrate (Millipore, Cat. WBKLS0500) was layered onto the membrane, and then the signal was detected using an Amersham Imager 600.

2.6. Collection of bronchoalveolar lavage fluid (BALF)

BALF were collected by performing consecutive washes of the airspace of the lungs of individual experimental mice, with 1.0 mL of sterile PBS (pH 7.4). The samples obtained were stored in a −80 °C freezer until tested for their contents of specific proinflammatory cytokines.

2.7. Enzyme-linked immunosorbent assay (ELISA)

The SARS-CoV-2 spike protein (GenScript, Z03481-100) was coated onto a 96-well microplate at 50 ng per well (Corning, Cat. 9018) overnight at 4 °C. The uncoated spike protein was removed, and the wells were blocked with 200 µl of blocking buffer (1× PBS with 1% BSA) for 2 h at room temperature. The plates were washed with 200 µl of PBS-T three times and added with 100 µl of diluted serum and incubated at room temperature for 2 h. The plates were washed with 200 µl of PBS-T three times, 10000-fold diluted HRP-conjugated donkey anti-mouse IgG, HRP-conjugated rabbit anti-mouse IgG1, and IgG2a antibodies (Invitrogen, Cat. 31430) were added to the wells and incubated for 1 h. The plates were washed with 200 µl of PBST. TMB substrate (Seracare, Cat. 5120–0077) was used at 100 µl per well and incubated for 10 min at room temperature. The reaction was halted with 100 µl of 2 N H_2SO_4. The optical density (O.D.) measurements were determined at 450 nm using a microplate reader. The endpoint serum dilution was calculated using the O.D. values and the cutoff value of serially diluted sera was set to three-fold the background signal. For detection of anti-Ad antibody, 100 µl of diluted serum from the immunized hamster were added into the 96-well microplates which were pre-coated with 1×10^6 pfu per well of heat-inactivated Ad-VR5 (wild type of Ad5 strain) and then blocked with blocking buffer. 10,000-fold diluted HRP-conjugated rabbit anti-hamster IgG antibody (Arigo, Cat. ARG23730) were added to the wells. After washing wash PBS-T, TMB substrate was added to the wells and then measured the OD at 450 nm using a microplate reader.

ELISA kit specific to mouse IFN-γ, IL-1, IL-2, and IL-4 (Thermo-Fisher Scientific, Cat. 88–7314-88, 88–5019-88, 88–7024-88, and 88–7044-88, respectively) were used. The limitation of each cytokine detection was 15 pg (IFN-γ), 4 pg (IL-1), 2 (IL-2), and 4 pg (IL-4), respectively. 100 µl/well of capture antibodies specific to cytokine were added into 96-well plate and then incubate at 4 °C for overnight. The plate was washed 3 times with 200 µl/well PBS-T

and then blocked with 200 µl/well ELISA/ELISPOT Diluent (1×) Buffer at room temperature for 1 h. After washing 3 times with PBS-T, 100 µl/well of BAL fluid or the respective recombinant cytokine standard protein was added to wells and incubate at room temperature for 2 h. The plate was washed again with PBS-T and added with 100 µl/well the respective detection antibody to all wells and incubated at room temperature for 1 h. The plate was washing again with PBS-T and 100 µl/well of diluted Streptavidin-HRP was added and incubated at room temperature for 30 min. The plates were washed forth with PBS-T and added with TMB substrate to react for 15 min. Reaction was halted with stop solution and the O.D. measurements were determined at 450 nm.

2.8. Neutralizing assay

One hundred microliters of serially diluted serum (reconstituted with preimmunized normal mouse serum to equal amounts of serum) was mixed with 200 $TCID_{50}$/100 µl of SARS-CoV-2 and incubated for 2 h at 37 °C. The mixture was then added to 2.4×10^4 Vero cells in a 96-well plate, and each dilution was repeated four times. Vero cell cultures that had been treated with the same dose of virus without sera were used as a positive control. Five days later, the CPE of the cells was visualized by microscopy at the set point of the diluted-fold sera according to the calculation of the titer of neutralizing antibody possessed by the sera.

2.9. Enzyme-linked immunoSpot assay (ELISPOT)

RBC-free splenocytes (5×10^5) prepared from individual mice were seeded into each well of the 96-well filtration plates (Millipore, Cat. S2EM004M99) precoated with 0.5 µg/well of monoclonal capture antibodies against murine IL-4 (BD, Cat. 551878) or IFN-γ (BD, Cat. 551881), and then subjected to ELISPOT assays [32]. 3-amine-9-ethylcarbazole (AEC; Sigma-Aldrich, Cat. AEC101-KT) substrate was added to react for cytokine-specific immunospot generation. The generated spots were scored using an immunospot counting reader (Immunospot, Cellular Technology Ltd.). The obtained number of spots was then subtracted to the number of spots gained from the respective well without restimulation (medium only). The results are expressed as the number of cytokine-secreting cells per 5×10^5 splenocytes seeded in the initial well, and the assay limit is higher than 1 cytokine-secreting cell per 5×10^5 splenocytes.

2.10. Flow cytometry

RBC-free splenocytes (5×10^5) from vaccine-immunized BALB/c mice were harvested and seeded into the 96-well plate. Splenocytes were co-cultured with or without nCoV recombinant spike protein (GenScript, Z03481-100) for 24 or 48 h to detect IFN-$\gamma^+CD3^+CD4^+$ cells or IL-4$^+CD3^+CD4^+$ cells, respectively. The stimulated splenocyte were pretreat with brefeldin A (TONBO, Cat. TNB-4506), phorbol 12-myristate 13-acetate (PMA) (5 ng/ml), and ionomycine (0.5 µg/ml) for 6 h before cell harvesting. The cells were stained with Zombie yellow viability kit (1:200, Biolegend, Cat. 423104) and incubated in the dark for 20 min at RT. Cells were wash two times with 1 %BSA PBS, and then added Fc block-CD16/CD32 monoclonal antibody (1:100, ThermoFisher, Cat: 14–0161-85) and stayed in the dark 15 min at 4℃. Cells were extracellularly stained with APC anti-mouse CD3 (Elabscience, Cat. E-AB-F1013UE) and PE-Cyanine5 anti-mouse CD4 (eBioscience, Cat. 15–0042-82). After washing, cells were fixed with 100 µl IC Fixation Buffer (ThermoFisher, Cat. 00–8222-49) for overnight at 4 °C. After fixation, cell permeabilized with Permeabilization buffer (ThermoFisher, Cat. 00–8333-56) and then washed two times. Cells

were intracellularly stained with FITC anti-mouse IFN-γ (1:200, Biolegend, Cat. 505806) and PE anti-mouse IL-4 (1:200, Biolegend, Cat. 504104) antibody. After washing two times, stained samples were analyzed by Attune NxT Flow Cytometer (ThermoFisher).

2.11. Statistical analysis

One-way ANOVA test was used to analyze the results from Figs. 2, 3B, 3C, 3D, 5, 5B, 5C, 6, and 9C. Two-way ANOVA test was used to analyze the results from Figs. 3A, 5D, and 9B. A nonparametric Mann-Whitney test was used to analyze the results from Figs. 4, 7, and 8. The results were considered statistically significant when P < 0.05. The symbols *, **, and *** are used to indicate P < 0.05, P < 0.01, and P < 0.001, respectively.

3. Results

3.1. Expression of S and SdTM of SARS-CoV-2 in Ad-infected cells

We had constructed an Ad5 genome that carried the full-length and transmembrane-deleted S genes of the SARS-CoV-2, AdCoV2-S and AdCoV2-SdTM (Fig. 1A). To detect the expression of spike protein in Ad-infected cells, the immunoblotting of the culture medium and lysates with anti-S antibody was performed. The bands located at ~185 kDa and ~182 kDa corresponded to S- and SdTM-expressed proteins, respectively, and some degraded S proteins were detected in the cytosolic fraction of the lysates. An additional band located at ~130 kDa which could be a cleavaged form of STM observed in AdCoV2-SdTM-expressed protein (Fig. 1B and supplementary Fig. 1A). S and SdTM were also detected in the membrane fraction of the lysate (Fig. 1C and supplementary Fig. 1B). However, only SdTM was detected in the Ad-infected culture medium (Fig. 1D and supplementary Fig. 1C). No signals were detected in any of the Ad-LacZ-infected samples (Fig. 1B, C, D). β-actin, ATP1A1, and mouse IgG heavy chain (supplementary Fig. 1A, 1B, and 1C, respectively) were detected independently as sample controls. These results indicated that either intact S or SdTM could be expressed in the respective Ad vector-infected cells. In addition, the membrane-deleted S that formed as a secretory protein was expected.

3.2. Induction of SARS-CoV-2-specific antibody responses by AdCoV2 vaccines

To investigate the immunogenicity of AdCoV2-S and AdCoV2-SdTM *via* systemic or mucosal administration, we immunized i.n. or s.c. BALB/c mice with 1×10^7 pfu of AdCoV2s on days 1 and 14. The sera were serially collected at 2 weeks and 1, 2, and 3 months after the second immunization. The anti-SARS-CoV-2 IgG response and the binding titer in the sera were analyzed. The specific IgG antibody was significantly detected as early as 2 weeks (titer = 12,800–25,600; Fig. 2A) and increased at one month (titer = 204,800; Fig. 2B), reaching its peak at the 2nd month (titer = >409,600; Fig. 2C) and then maintaining the antibody level at the 3rd month (titer = 409,600; Fig. 2D) in AdCoV2-S-immunized i.n. serum. The antibody titers were 3200, 25,600, 102,400, and 25,600 at 2 weeks and 1, 2, and 3 months, respectively, in the AdCoV2-SdTM-immunized i.n. serum. Antibody titers of 6400, 25,600, 51,200, and 25,600 were detected in the AdCoV2-S-immunized s.c. serum at 2 weeks and 1, 2, and 3 months, respectively. No anti-SARS-CoV-2 IgG was detected at any of the time points in the Ad-LacZ-immunized serum (Fig. 2). In parallel, SARS-CoV-2-specific IgA was observed in the mucosal site of the vaginal wash (vw), which was collected from the mice immunized i.n. with AdCoV2-S at 2 weeks and 1 month after the second immu-
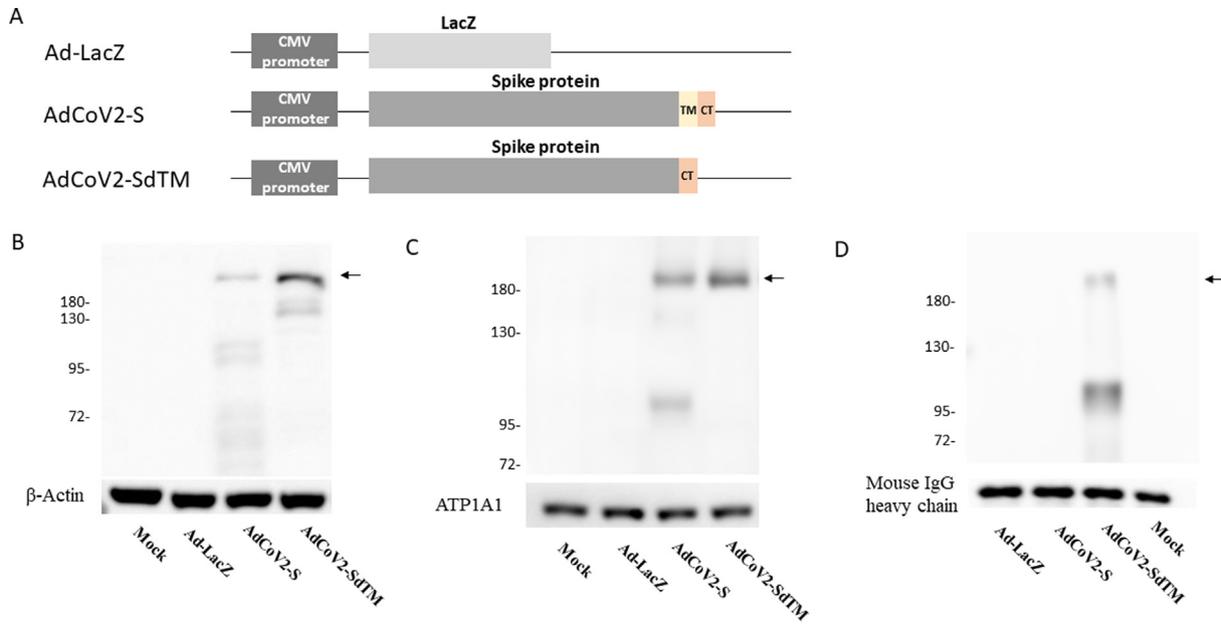
Fig. 1. Construction and analysis of SARS-CoV-2 spike expression in AdCoV2 vaccines AdCoV2-S and AdCoV2-SdTM were constructed as described in the Materials and Methods, and their brief genetic maps are shown (A). Uninfected 293 cells (mock) and cells infected individually with Ad-LacZ, AdCoV2-S, and AdCoV2-SdTM at an MOI of 0.1 for 24 h were used. Parts of the culture medium (D) and the lysate were harvested. Lysates were extracted to obtain cytosolic (B) and membrane (C) fractions as described in the Materials and Methods. The prepared samples (B, C, and D) were mobilized in SDS-PAGE electrophoresis and antigenically transferred onto the western blot membrane, then blotted with S-specific antibodies, (B and C) Mab5 or (D) COVID-19, 2019-nCoV. The target proteins marked by arrow were shown. Specific antibodies against β-actin, ATP1A1, and mouse IgG heavy chain were used as sample controls for the immunoblots of the cytosolic fraction, membrane fraction, and culture medium, respectively. The data are representative of the results derived from two independent experiments.
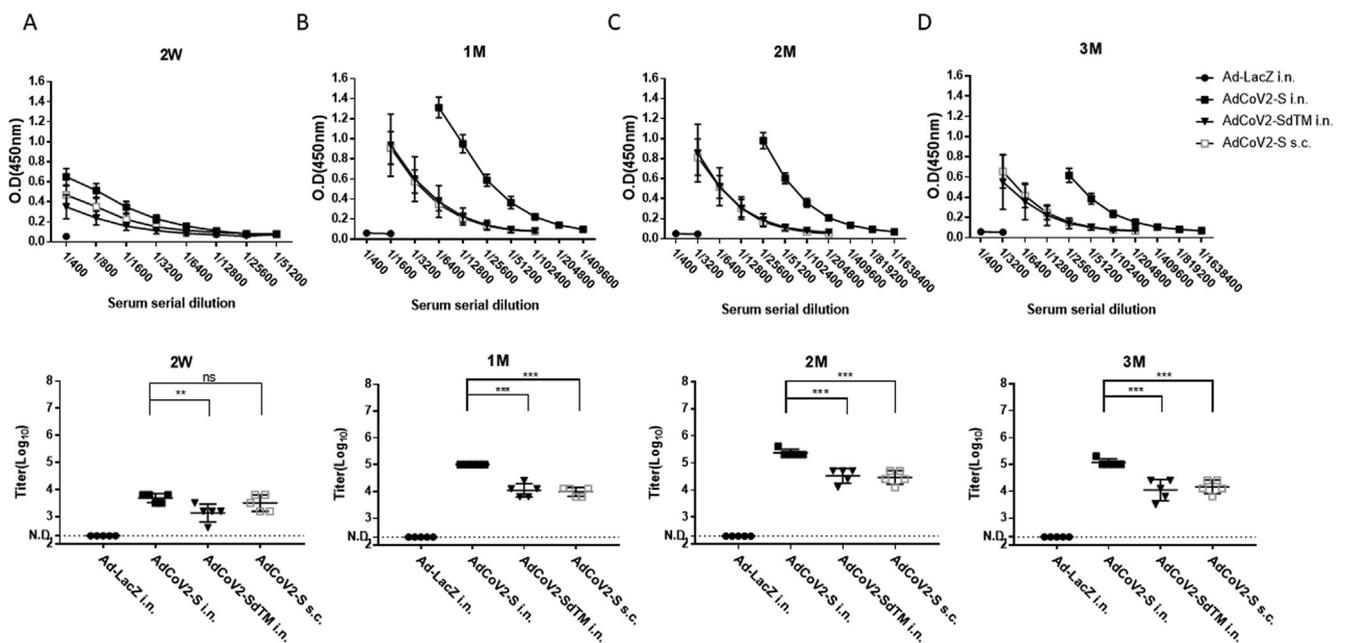

Fig. 2. Induction of SARS-CoV-2-specific IgG by AdCoV2 vaccines. Five mice per group of BALB/c were immunized with 1×10^7 pfu Ad-LacZ, AdCoV2-S, or AdCoV2-SdTM *via* i.n. or AdCoV2-S *via* s.c., five mice per group at 14-day intervals. The varying dilutions of sera collected at 14 days (A) or 1 (B), 2 (C), or 3 (D) months post boost were analyzed using IgG anti-recombinant intact S protein-immobilized ELISA. Anti-mouse IgG conjugated with HRP was used as the detection antibody. The titer of specific antibody in the serum was calculated as a fold dilution of the tested sera, whose detected value at OD450 nm of absorbance > 3 times the value at OD450 nm of absorbance obtained from the medium alone.

nization, compared to the lower level of SARS-CoV-2-specific IgA found in the vw obtained from the AdCoV2-SdTM-immunized i.n. mice. The vw from AdCoV2-S s.c. or Ad-LacZ i.n.-immunized mice did not have SARS-CoV-2-specific IgA (Fig. 3A). We also detected SARS-CoV-2-specific IgA in BALF at 6 days after the second immunization. Similarly, IgA was detected in the BALF from AdCoV2-S i.

n. and AdCoV2-SdTM i.n.-immunized mice, but not found in the BALF from AdCoV2-S s.c. and Ad-LacZ i.n.-immunized mice. In which higher level of IgA was found in the AdCoV2 i.n. group, compared to the AdCoV2-SdTM i.n. group (Fig. 3B).

A higher or lower antigen-specific IgG1/IgG2a ratio in immunized sera that represented an immune response biased to Th2-
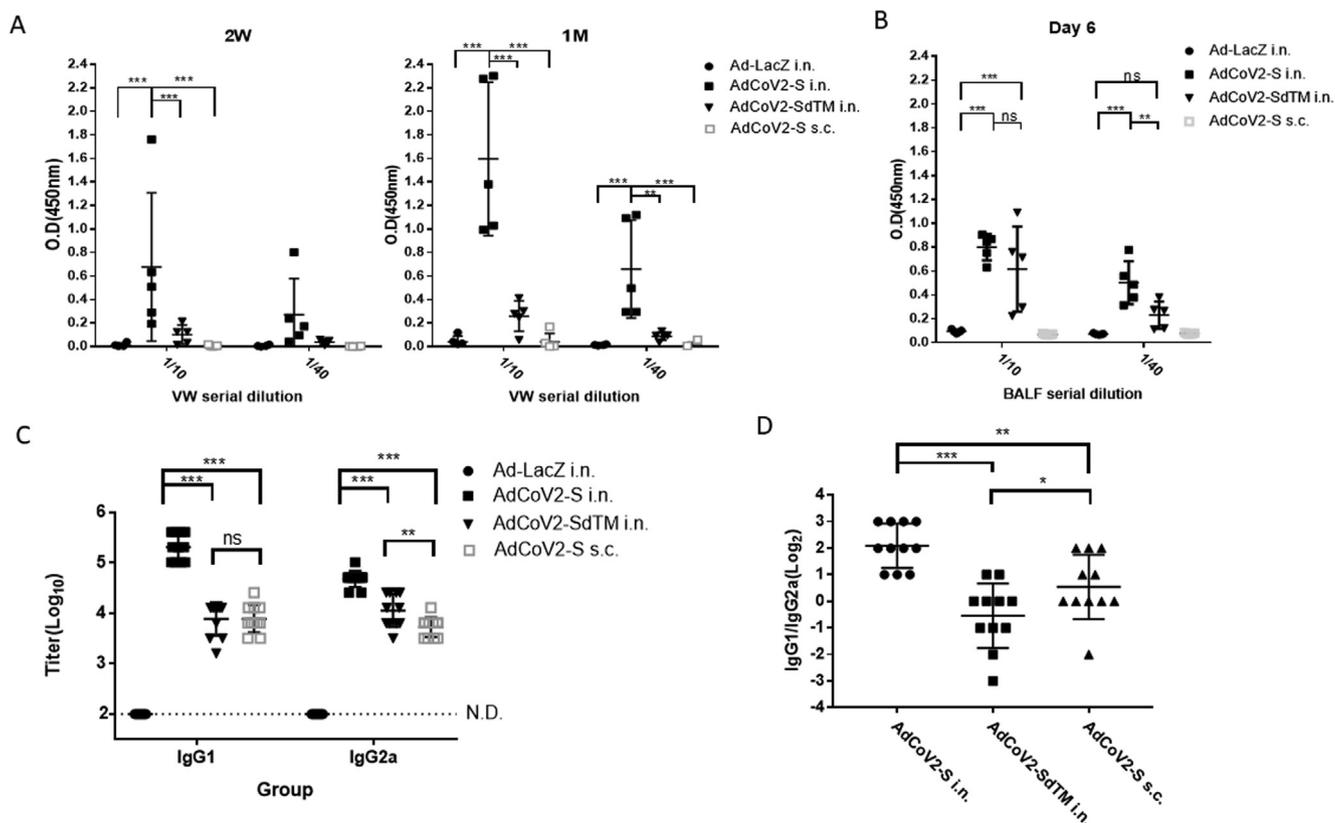
Fig. 3. Induction of the anti-SARS-CoV-2 IgA and IgG subclass by AdCoV2 vaccines. Sera and vw from BALB/c immunized twice with 1×10^7 pfu Ad-LacZ, AdCoV2-S, or AdCoV2-SdTM *via* i.n. or AdCoV2-S *via* s.c. at 14-day intervals were set to detect the subclass of specific Ig. (A) vw was collected at 14 days or 1 month and (B) BALF was collected at 6 days after the second immunization. 1/10 or 1/40-diluted individual vw and BALF were then subjected to recombinant intact S protein-immobilized ELISA for IgA detection. For SARS-CoV-2-specific (C) IgG1 IgG2a detection, diluted immune sera were examined using recombinant intact S protein-immobilized ELISA. Anti-mouse IgG1 or IgG2a conjugated with HRP was used as the detected antibody. (D) The ratio of IgG1/IgG2a based on the titer obtained from (B) was calculated. The results from 2 independent experiments were combined and presented. Eleven mice per group were included.
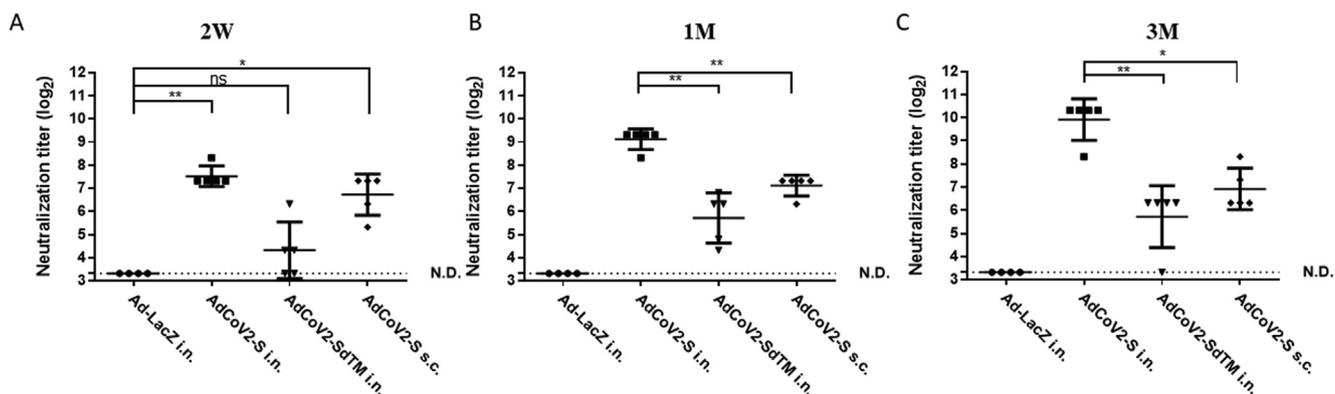

Fig. 4. Induction of neutralizing antibody against SARS-CoV-2 by AdCoV2 vaccines. BALB/c mice were immunized with 1×10^7 pfu Ad-LacZ (N = 4), AdCoV2-S (N = 5), or AdCoV2-SdTM (N = 5) *via* i.n. or AdCoV2-S (N = 5) *via* s.c. at 14-day intervals. Sera collected from AdCoV vaccine-immunized BALB/c mice at 14 days (A), 1 month (B), and 3 months (C) post-immunization were applied to the neutralizing assay which was described in the Materials and Methods. N represents as numbers of mice per group. The experimental protocol was followed for the regulation of the RG-3 level during laboratory operation.

mediated humoral or Th1-mediated cellular immunity, respectively, was reported [33]. SARS-CoV-2-specific IgG1 and IgG2a from all the AdCoV-2 vaccine sera were detected, in which the high to low sequence of IgG1 were AdCoV-2-S i.n. > AdCoV2-S s.c. ≈ AdCoV2-SdTM-S i.n., but IgG2a levels were AdCoV-2-S i.n. > AdCoV2-SdTM-S i.n. > AdCoV2-S s.c. (Fig. 3B). A higher IgG1 titer than that of IgG2a was significantly induced in the i.n. groups administered AdCoV2-S, but a similar amounts of IgG1 and IgG2a was observed in the AdCoV2-S s.c., and AdCoV2-

SdTM-S i.n. (Fig. 3B). Therefore, the IgG1/IgG2a ratio from individual samples was calculated, and we found that AdCoV2-S i.n. induced a higher ratio score ($2.1\log_2$) than AdCoV2-S s.c. ($0.55\log_2$). The lowest ratio score ($-0.55\log_2$) was found in AdCoV2-SdTM i.n. (Fig. 3C). This finding reveals that different immunization routes might affect the immune reaction, whereas AdCoV2-S i.n. immunization favors the Th2-mediated antibody response, in contrast to Th1 response, which are favored by AdCoV2-S s.c. immunization.
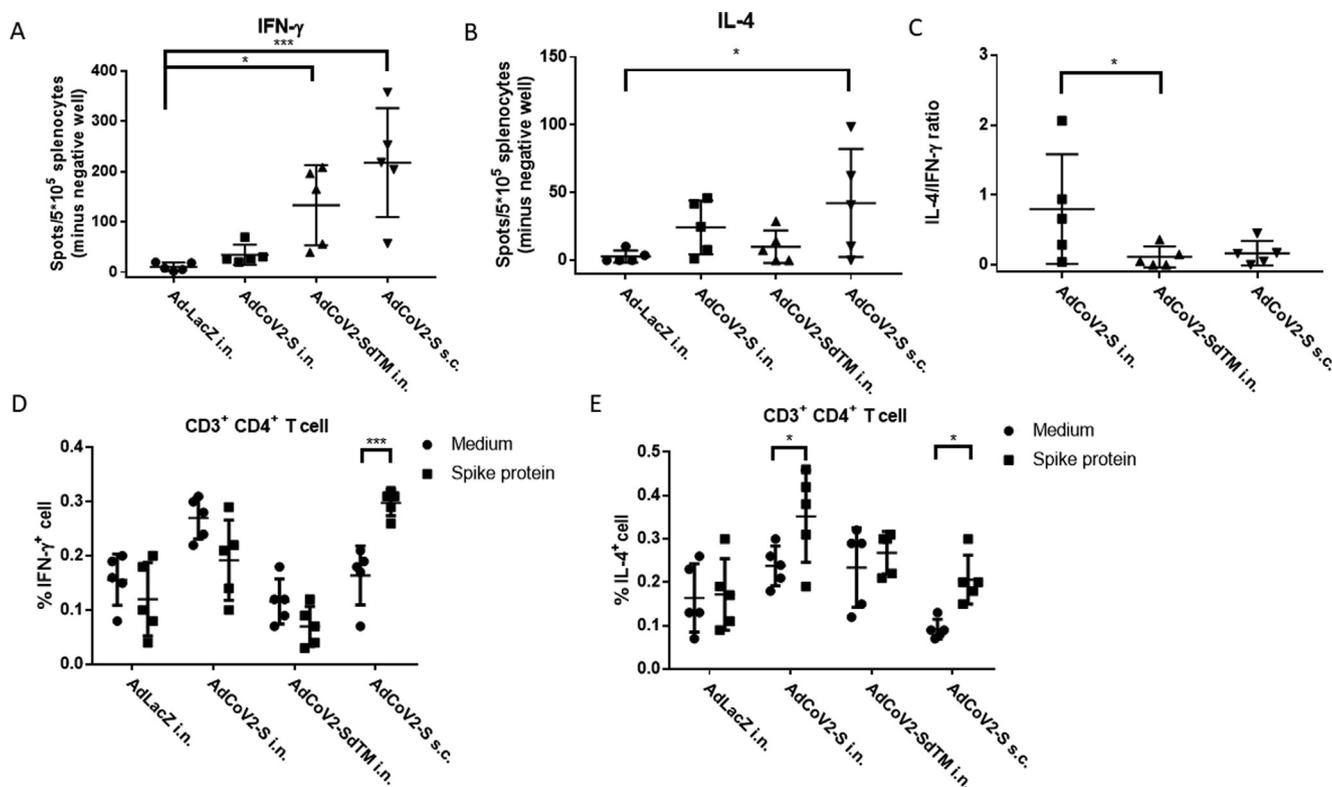
Fig. 5. Induction of SARS-CoV-2-specific cellular immunity by AdCoV2 vaccines. Five mice per group of BALB/c were individually primed and boosted at 14-day intervals though i.n. or s.c. routes with 1×10^7 pfu of AdCoV2 or Ad-LacZ. Ad-immunized mice were sacrificed 3 months after the vaccine boost, and splenocytes were collected and cultured in the presence or absence of 10 µg/mL S protein or 10 µg/ml Con A. A total of 5×10^5 splenocytes were seeded on (A) anti-IFN-γ or (B) anti-IL-4 capture antibody-coated ELISPOT plates for 24 or 48 h, respectively, for the ELISPOT assay. Cytokine-positive spots were developed, and the obtained number of spots from S-stimulated lymphocytes was then subtracted to the number of spots gained from the respective well with medium only. The results are expressed as the number of spots for each mice in the experimental group. (C) The ratio of IFN-γ-positive spot numbers/IL-4-positive spot numbers was calculated and shown. Two independent experiments were performed and one of the representative data was shown. In parallel, the results regarding the percentage of (D) IFN-γ$^+$ or (E) IL-4$^+$ populations in CD3$^+$CD4$^+$ splenocytes with or without S protein restimulation were shown. The method was described in the section of Materials and Methods. Briefly, S-stimulated splenocytes were double stained with anti-CD3 and anti-CD4 antibodies conjugated with APC and PE-Cyanine5- dye, respectively. After fixation and permeabilization, splenocytes were stained with (D) FITC-conjugated IFN-γ-specific antibody or (E) PE-conjugated IL-4-specific antibody. The 3-coloured splenocytes were individually analyzed by flow cytometry.

3.3. Neutralizing antibody against SARS-CoV-2 induced by AdCoV2 immunization

We further examined the SARS-CoV-2-specific neutralizing antibody induced by AdCoV2 immunization. Sera collected from AdCoV2-immunized i.n. or s.c. BALB/c mice at 2 weeks and 1 and 3 months after the second immunization were subjected to the SARS-CoV-2 neutralizing assay based on TCID$_{50}$, which was described in the Materials and Methods. The neutralizing antibody was detected as early as 2 weeks later in serum from the AdCoV2-S and AdCoV2-SdTM groups, in which the titer of anti-SARS-CoV-2 antibody was approximately 192, 24, 120, and 0 (the limitation of TCID$_{50}$ assay = 20) in the serum from the AdCoV2-S i.n., AdCoV2-SdTM i.n., AdCoV2-S s.c., and vector control Ad-LacZ i.n. groups, respectively (Fig. 4A). After that, the neutralizing antibody was increased and the titers were approximately 576, 56, 144, and 0 in the 1-month serum from the AdCoV2-S i.n., AdCoV2-SdTM i.n., AdCoV2-S s.c., and Ad-LacZ i.n. groups, respectively (Fig. 4B). The titers were steadily increased to approximately 1088, 64, 144, and 0 in the 3-month serum from the AdCoV2-S i.n., AdCoV2-SdTM i.n., AdCoV2-S s.c., and Ad-LacZ i.n. groups, respectively (Fig. 4C). These results indicated that neutralizing antibodies against SARS-CoV-2 could be effectively induced and reached a peak at 3 months post vaccination with AdCoVs. The increase in protective antibodies elicits a long-term pattern in AdCoV2-immunized subjects. This finding is consistent with the SARS-CoV-2 binding activity results showing that AdCoV2-S possesses stronger immunogenicity than AdCoV-2-SdTM in inducing the

anti-SARS-CoV-2 antibody response. In addition, the i.n. route is better than the s.c. route for AdCoV2 immunization.

3.4. Induction of Th1/Th2-mediated cellular immunity by the AdCoV2 vaccine

Cellular immunity is important for providing protective efficacy during the development of SARS-CoV-2 vaccines [34]. To examine which type of cellular immunity was induced by AdCoV2 vaccines, splenocytes were isolated from the Ad-immunized spleen at 3 months after the boost, followed by in vitro restimulation with medium only or recombinant S from SARS-CoV-2, and then assayed for cytokines by ELISPOT. S-stimulated lymphocytes from Ad-LacZ i.n.-immunized mice produced background IFN-γ levels. By contrast, the highest IFN-γ levels were detected in S-stimulated lymphocyte cultures from AdCoV2-S s.c.-immunized mice and moderate levels in AdCoV2-SdTM i.n. and the lowest levels in AdCoV2-S i.n.–immunized mice (Fig. 5A). Within the panel of Th2 cytokines that were assayed, IL-4 was most highly secreted by lymphocytes from AdCoV2-S s.c.-immunized mice compared to moderate levels in AdCoV2-S i.n.- and the following AdCoV2-SdTM i.n.-immunized mice (Fig. 5B). The IL-4/IFN-γ ratio was also calculated, and the mean of ratio score obtained from AdCoV2-S i.n. group was 0.80. It was higher than that of the AdCoV2-S s.c group (0.17) and AdCoV2-SdTM i.n. group (0.11) (Fig. 5C). Furthermore, CD3$^+$CD4$^+$ T cells were isolated from S-stimulated or unstimulated lympnocytes. The IFN-γ$^+$ and IL-4$^+$ populations within the isolated lymphocytes were intracellularly
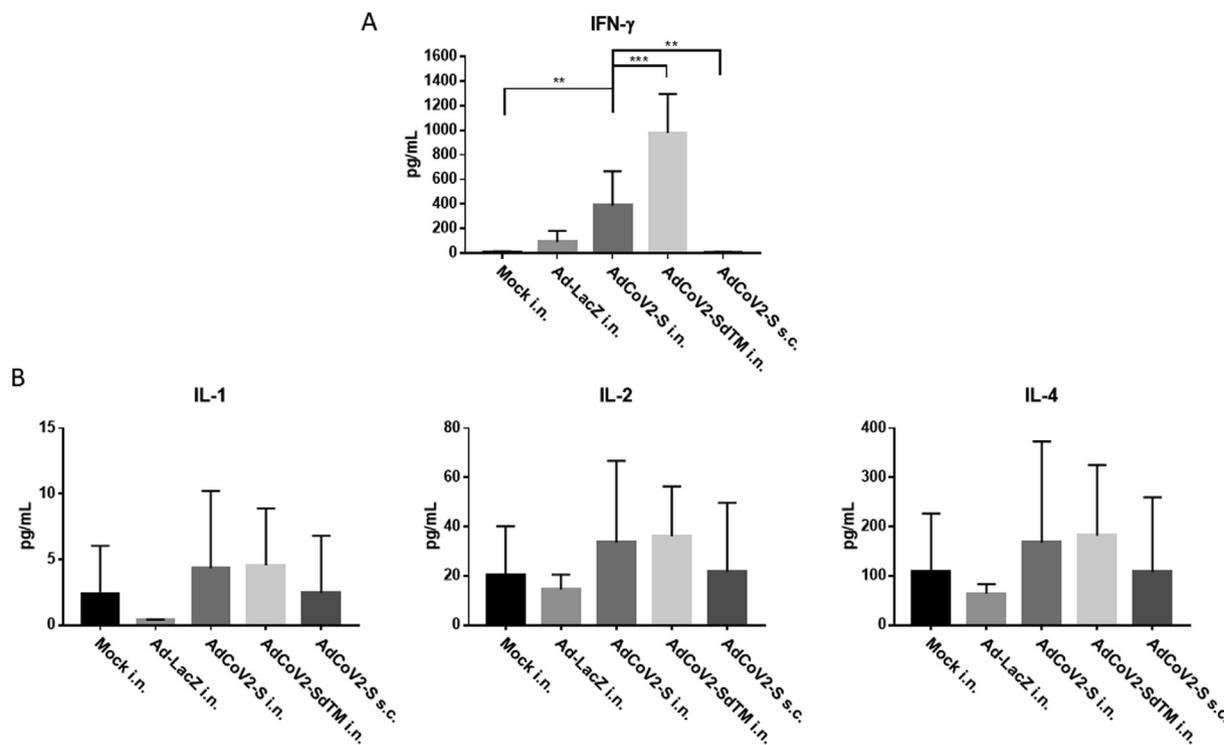
Fig. 6. Detection of proinflammatory cytokines in the AdCoV2-immunized BALF BALF from individual mice immunized twice via i.n. route with Ad-LacZ, AdCoV2-S, or AdCoV2-SdTM, or s.c. route with AdCoV2-S, five mice per group, were quantitated for their contents of (A) IFN-γ and (B) IL-1, IL-2 and IL-4, using the reagents and protocols that were described in the Material and Methods. Results are presented as the concentration of the cytokine in pg per mL.

stained with the respective antibody conjugated with fluorescence dye and then analyzed by flow cytometry. The populations IFN-γ^+CD3$^+$CD4$^+$ T cells were significantly increased in AdCoV2-S s.c.-immunized mice, compared to non-significant change of IFN-γ^+CD3$^+$CD4$^+$ T cells in AdCoV2-S i.n. and AdCoV2-SdTM i.n.-immunized mice after S antigen stimulation. (Fig. 5D). Consistently, the higher populations of IL-4$^+$CD3$^+$CD4$^+$ T cells were detected in AdCoV2-S i.n.-immunized mice and AdCoV2-S s.c.-immunized mice as well (Fig. 5E). Both of IFN-γ^+ CD3$^+$CD4$^+$ and IL-4$^+$ CD3$^+$CD4$^+$ T cell populations were shown no any change in Ad-LacZ i.n.-immunized mice after S antigen stimulation (Fig. 5D and 5E). It thereby indicate that AdCoV2-S i.n. group elicited Th2 activation biasedly, in contrast to both of AdCoV2-S s.c. and AdCoV2-SdTM i.n. that skewed cellular response to Th1.

To further examine the secretion of proinflammatory cytokines in the lung by AdCoV2 vaccine immunization, DMEM medium (Mock) or AdCoV2-immunized mice were sacrificed, and individual BALFs were prepared on 1 week after the two-dose immunization for detecting the secretion of proinflammatory cytokines. IFN-γ was significantly induced in the BALF from AdCoV2-S in. and Ad-CoV2-SdTM i.n.-immunized groups but was not induced in the BALF from AdCoV2-S s.c. or Ad-LacZ i.n.. It indicates that i.n. delivery of AdCoV2 vaccine can induce Th1-biased responses in the lungs (Fig. 6A). IL-1, IL-2, and IL-4 (Fig. 6B) were measured and all of them were not induced after Ad vaccines immunization. The amounts of these cytokines were detected as background level as Mock group, suggesting that s.c. and i.n. of AdCoV2 vaccine did not induce the proinflammatory cytokines except IFN-γ in the respiratory tract.

3.5. Potency of AdCoV2 vaccine in protection against SARS-CoV-2 infection

A previous study showed that hamsters were an animal model for SARS-CoV and SARS-CoV-2 [35]. Therefore, we assessed the protective effect of AdCoV2 vaccines against SARS-CoV-2 in this animal model. Because of the limitation for SARS-CoV2 resources and ABSL-3 operation capacity, we performed only the protection 1-month post-infection study. Administration of AdCoV2-S or AdCoV2-SdTM *via* the i.n. route (Exp. 1) or AdCoV2-S i.n. *vs.* AdCoV2-S s.c. (Exp. 2) in hamsters following a challenge with live SARS-CoV-2 was performed paralleled. The animals were then sacrificed, and the pulmonary viral loads and lung tissue sections and histochemical staining were examined at days 3 and 6 post-viral challenge. On day 3 post-challenge, there was significant inhibition (10^4–10^3-fold reduction) of SARS-CoV-2 in the lungs of hamsters that were immunized with AdCoV2-S i.n. or AdCoV2-SdTM i.n. in comparison to Ad-LacZ-vaccinated tissues that contained high amounts of SARS-CoV-2 (Exp. 1, Fig. 7A). Compared to the most inhibition ($10^7 \sim 10^4$-fold reduction) inducted by AdCoV2-S i.n., mild inhibition (10^3–10^1-fold reduction) was observed in AdCoV2-S s.c. immunization (Exp. 2, Fig. 7A). On day 6 post-challenge, no (lower than the detection limit) SARS-CoV-2 was detected in AdCoV2-S i.n.- and AdCoV2-SdTM i.n.-immunized lungs compared to some virus (10^3 TCID$_{50}$/mL) that was detected in Ad-LacZ-immunized lungs (Exp. 1, Fig. 7B). Similarly, very few SARS-CoV-2 were detected in the group of AdCoV2-S i.n. or AdCoV2-S s.c., respectively, compared to virus (10^5 TCID$_{50}$/mL) detected in Ad-LacZ-immunized lungs (Exp. 2, Fig. 7B). Additionally, Ad-LacZ was not able to prevent SARS-CoV-2-induced weight loss, while AdCoV2-S i.n. and AdCoV2-SdTM i.n. could prevent weight loss in hamster (Exp. 1, Fig. 7C). Compared to AdCoV2-S i.n., AdCoV2-S s.c. also showed some activity in preventing weight loss, even though no significant difference was observed (Exp. 2, Fig. 7C).

To evaluate the inhibition of SARS-CoV-2-induced lung inflammation and the safety of AdCoV2 vaccine administration in animals upon viral infection, we examined the lung pathogenesis of hamsters immunized with AdCoV2-S i.n. *vs.* AdCoV2-SdTM i.n. (Exp.1) or AdCoV2-S i.n. *vs.* AdCoV2-S s.c. (Exp. 2) followed by SARS-
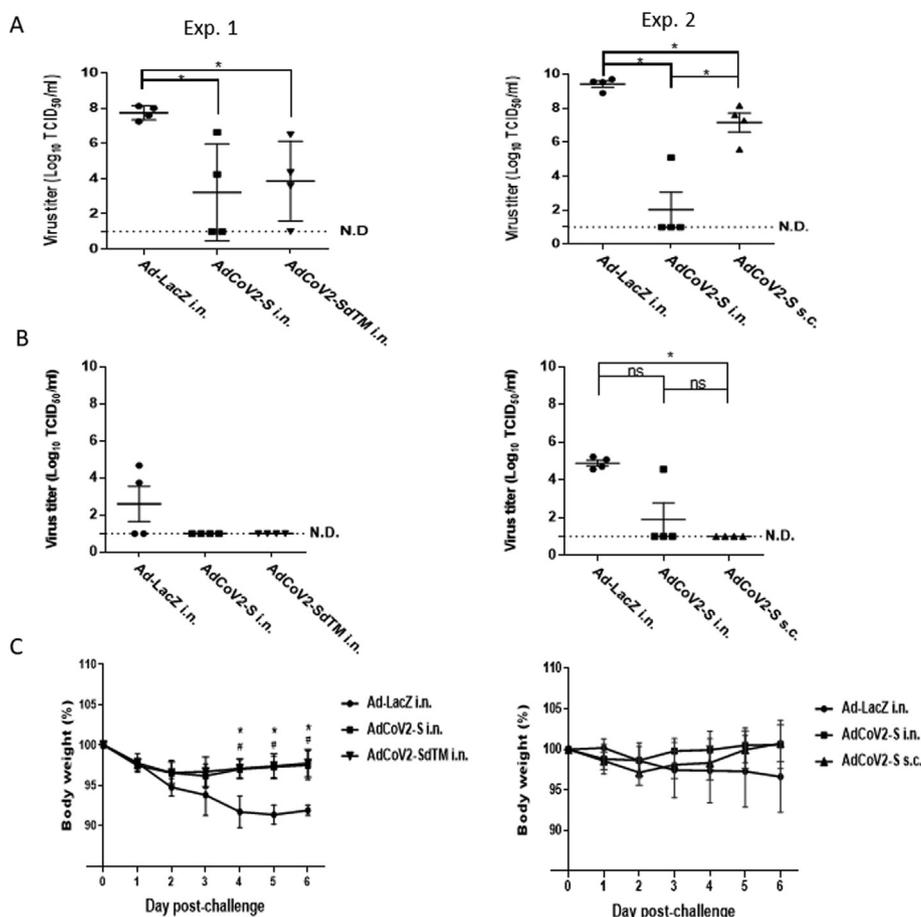
Fig. 7. AdCoV2 vaccines protect animals from SARS-CoV-2 infection. Four hamsters per group were preimmunized twice i.n. with 3×10^7 pfu Ad-LacZ i.n., AdCoV2-S i.n., AdCoV2-S s.c., or AdCoV2-SdTM i.n. over a 14-day interval and then infected i.n. with 1×10^5 pfu of live SARS-CoV-2 1 month after the second vaccine shot. (A) On days 3 and (B) 6 post-infection, the hamsters were sacrificed and the lung tissues were homogenized for the $TCID_{50}$ assay. The lowest limitation of detection for $TCID_{50}$ assay was 1×10^1 $TCID_{50}$/mL. (C) The body weight of AdCoV2-immunized hamsters followed by SARS-CoV-2 challenge was recorded. The results from 2 independent experiments (Exp. 1 and 2) were presented separately. When Ad-LacZ i.n. compares with AdCoV2-S i.n., the symbols * are used to indicate P < 0.05. When Ad-LacZ i.n. compares with AdCoV2-SdTM i.n. and AdCoV2-S s.c., the symbols # are used to indicate P < 0.05.

CoV-2 infection. H/E-stained lung tissues from Ad-LacZ-immunized hamsters showed severe inflammation associated with lymphocyte infiltration among the alveoli, as expected (Exp. 1 and 2, Fig. 8A). Mild inflammation was found in AdCoV-S i.n.-immunized tissues and mild to moderate inflammation was observed in AdCoV-SdTM i.n.-immunized tissues (Exp. 1, Fig. 8A). Compared to AdCoV-S i.n., even very mild inflammation was found in AdCoV-S s.c.-immunized lung sections (Exp. 2, Fig. 8A). We scored the degree of inflammation in the lungs of each visualized section. The sections from Ad-LacZ i.n.-immunized mice exhibited the highest score (average = 3.75 and 2.75 in exp. 1 and exp. 2, Fig. 8B, respectively) for inflammation in the lung sections. By contrast, the lowest inflammation score (average = 0.875) was observed in AdCoV-S s.c.-immunized tissues (exp. 2, Fig. 8B). The similar degree of inflammation (average = 0.5 and 1.375 in exp. 1 and exp. 2, respectively, Fig. 8B) was observed in AdCoV-S i.n.-immunized tissues. A medium inflammation score (average = 3) was found in AdCoV-SdTM-immunized tissues (Exp. 1, Fig. 8B). These pathologic results was consistent to the protection study showing that AdCoV2-S was better than AdCoV2-SdTM at the reduction of viral amounts in the lungs. Additionally, AdCoV2-S was better than AdCoV2-SdTM at inhibiting SARS-CoV-2-induced lung inflammation and was safe during the immunization in animals.

3.6. The effect of pre-existing anti-Ad antibody in the induction of anti-S humoral responses by AdCoV2 vaccine

To investigator whether the pre-existing anti-Ad antibody could influence the immunogenicity of AdCoV2 vaccine in the induction of anti-S antibody response or not, we performed the intramuscular (i.m.) injection of 1.5×10^8 pfu of AdLacZ (PEI) to induce pre-existing anti-Ad antibody, and following priming/boosting (3×10^7 pfu per dose, 2-week interval) of AdCoV2-S i.n. or s.c. in hamster (Fig. 9A). The raising anti-Ad antibody were found (titer = $\sim 10 \log_2$) in PEI-injected mice at day 20 before Ad vaccine immunization. However, similar anti-Ad antibody level ($\sim 10 \log_2$) was detected in PEI + AdCoV2-S i.n. and PEI + AdCoV2-S s.c. groups at day 65 after two-dose of AdCoV2-S immunization. A lower level of anti-Ad antibody ($\sim 7.5 \log_2$) was observed in AdCoV2-S i.n. and AdCoV2-S s.c. groups without PEI-injection (Fig. 9B). Interestingly, the anti-S antibody from PEI + AdCoV2-S i.n. or PEI + AdCoV2-S s.c ($5 \log_{10}$, or $3 \log_{10}$, respectively) were all significantly induced and no any harm by pre-existing high level of serum anti-Ad antibody, compared to the similar titer of anti-S antibody detected in AdCoV2-S i.n. or AdCoV2-S s.c.-immunized groups without PEI pre-treatment ($5 \log_{10}$, or $3 \log_{10}$, respectively, supplementary Fig. 9C). In summary, mucosal delivery of the AdCoV2 vaccine has advantages of expressing full protection against SARS-CoV-2.
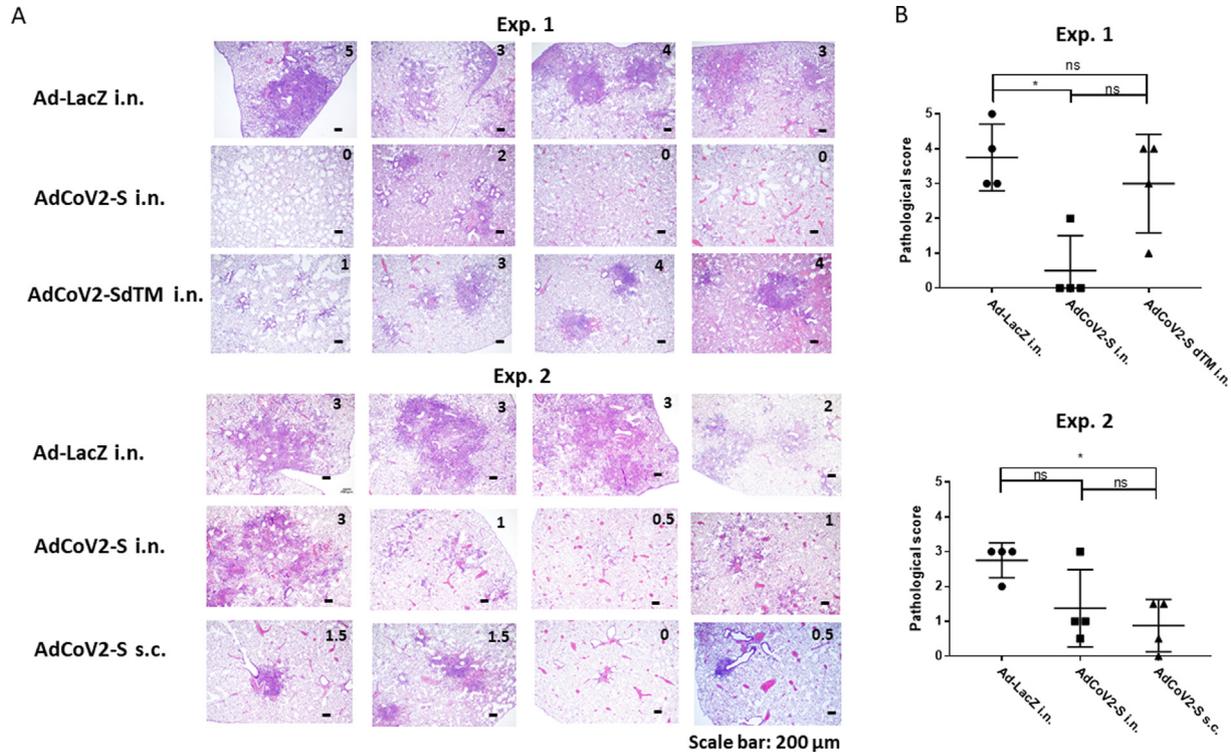
Fig. 8. Inhibition of lung inflammation induced in SARS-CoV-2-challenged hamsters by AdCoV2 vaccines. Sections of lung tissues collected from AdCoV vaccine-immunized hamsters on day 6 post-infection as described in the legend of Fig. 7 were stained with H/E dye. (A) A representation of the pictures of H/E-stained lung sections from each hamster is shown and the score of disease as judge by the criteria as described in the Materials and Methods is marked. (B) The severity of the histopathology in each section is graded and shown based upon the score. The results from 2 independent experiments (Exp. 1 and 2) were presented separately.
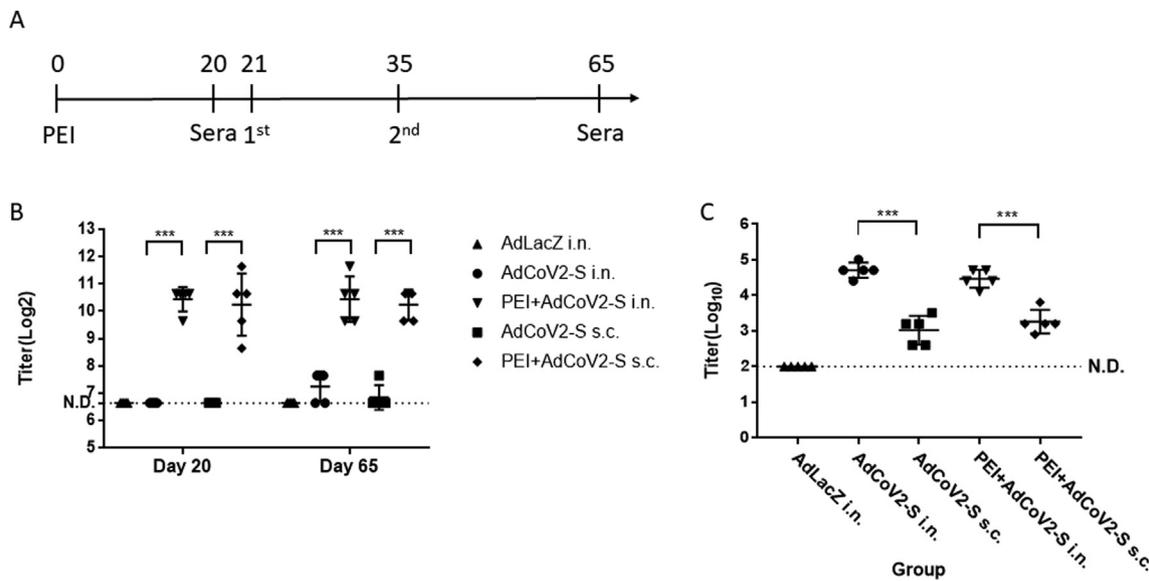

Fig. 9. Induction of pre-existing anti-Ad antibody following immunization of AdCoV2 vaccine in hamster. Hamster were pre-injected i.m. with 1.5×10^8 pfu of AdLacZ (PEI) at day 0 and then primed/boosted (3×10^7 pfu per dose, 2-week interval) with AdCoV2-S i.n. or s.c. at day 21 and day 35 after 3 weeks of PEI injection(A). Another group of hamster immunized with AdCoV2-S i.n. or s.c. without pre-treatment of PEI was included. The serum at day 20 before AdCoV2-S injection and at day 65 (post 1 month of AdCoV2-S immunization) were taken for subsequent (B) anti-Ad and (C) anti-S antibodies detection by ELISA that was described under the methods.

4. Discussion

Antibody-dependent enhancement (ADE) has been observed in coronaviruses, including SARS, MERS [36], and other human respiratory virus infections, such as RSV [37] and measles [38,39]. SARS-CoV prototype vaccines that induce a Th2-type immune response have a risk of ADE in animal models [40,41]. Thus, there is a suggested risk of ADE in SARS-CoV-2 vaccines and antibody-based interventions that should receive attention [36]. Recombinant replication-incompetent adenoviruses have an acceptable safety profile in humans and are able to induce neutralizing antibodies, CD4 and CD8 T cell responses and a Th1-biased immune response in animals and humans [42–45]. Recently, a study showed that

express wild-type or modified S protein by Ad5 *via* neither s.c. nor i.n. immunization was able to detect the IL-4⁺ T cell response[46]. However, our studies showed that AdCoV2s elicited strong antibody response (e.g., AdCoV2-S; Fig. 2) and activated the Th1 and Th2-comparable cellular immunity (e.g., splenic IFN-γ and Il-4 release and the populations IFN-γ⁺Th and IL-4⁺Th cells, respectively, shown in Fig. 5, and IgG2a and IgG1 induction, respectively, shown in Fig. 3) in response to AdCoV2-S and AdCoV2-SdTM. Moreover, we found that AdCoV2-S i.n. induced a better antibody response than s.c., but AdCoV2-S s.c. induced a better cellular immune response than i.n.. This result is consistent to the previous study which showed that Ad5-SARS-CoV2 i.m. is better than i.n. in cellular immune response in rhesus macaques [47]. Other studies showed that immunization of Ad5 expressing S1 or RBD domain (Ad-S1 or Ad-RBD, respectively) *via* i.n. also induced a good immunity against SARS-CoV2 in animal models[48,49]. Meanwhile, Ad-S1 or Ad-RBD s.c. induced a stronger cellular immunity[48]. Thus, what the mechanism of other subsets of Th (such as Tfh and Th17) activation involved in AdCoV2 vaccines immunization *via* different route that influence the differential immune response and long-term memory will be investigated in the future.

AdCoV2-SdTM induced a weaker neutralizing antibody response than AdCoV2-S (Fig. 4). Is it possible that the souble S (SdTM) which even elicited a stronger expression in cell culture (Fig. 2) is presented in the Ad-immunized serum and vw that might reduce the anti-S IgG and IgA titer? Indeed, we examined the presence of S antigen in Ad-immunized mouse serum and vw after 2 week of the second immunization by western blot. The results showed that S antigens were detected in neither AdCoV2-immunzed serum nor vw samples (Supplementary Fig. 2A and B, respectively). Another explanation that the intact S protein expressed by AdCoV2-S-infected cells might highly mimic the pre-fusion form of S protein on the viral particle that could activate an adequate host antibody to recognize and neutralize the natural virus. In other words, the structure could be changed after the deletion of the membrane domain from the S protein, which might induce inadequate antibodies and subsequently affect binding and neutralizing to the virus (Figs. 2 and 4, respectively). Mucosal administration (i.n.) of Ad-based vaccines is more immunogenic than systemic administration (s.c.) in the induction of antibody response, especially for respiratory infections. In fact, mucosal delivery of AdCoV2-S induced the dominant IgG and IgA (Figs. 2 and 3. Respectively), compared to the systemic administration of AdCoV2-S which induced IgG only. Clinical study reveals that IgA is dominated than IgG and IgM in the serum, saliva, and BALF of SARS-CoV2-infected patients. IgA peaks at 3 weeks after symptom onset but persists for several more weeks in saliva. Also, IgA is more potent than IgG in neutralizing SARS-CoV2 [50]. An Ad5-encoded influenza A/PR/8/34 hemagglutinin (HA) with an i.n. or epicutaneous injection route in humans was found to be safe and immunogenic for inducing the anti-HA antibodies. The intranasal vaccine of Ad-PR.8.HA was more potent than when administered epicutaneously [51]. However, the third event in this study reveals that AdCoV2-S administration *via* the i.n. or s.c. route, or AdCoV2-SdTM *via* the i.n. route, all showed sufficient efficacy in preventing SARS-CoV-2 infection, as evidenced by the effect on hamsters that were immunized following challenge with SARS-CoV-2 (Fig. 7).

Several pre-clinical studies have shown that mucosal but not systemic immunization with an Ad vaccine induced long-term immunity against pathogens, such as the Ad vector-expressing glycoprotein B of herpes simplex virus type 2 (HSV-2) against HSV-2 [52]. Long-lasting anti-respiratory syncytia virus (RSV) immunity was induced by a nasal Ad vector expressing the fusion protein Ad-RSV-F [53]. Our results also confirmed that the neutralizing antibody against SARS-CoV-2 induced by i.n. delivery of AdCoV2-

S was even continuously increased up to highest titer after three months of the second booster (Fig. 4).

Pre-existing anti-Ad host immunity is always an issue to track when assessing the efficacy of Ad-based vaccines. A high titer of anti-influenza HI antibody was induced in subjects who had a high pre-existing antibody titer to Ad by Ad-PR.8 HA vaccine immunization. This finding indicated that the Ad-PR.8. HA vaccine showed no correlation with pre-existing neutralizing antibodies to Ad and the potency of Ad vaccines in a human trial [51]. The high amount of serum pre-existing Ad antibody partially diminished both the SARS-CoV2-specific antibody response and CD4⁺ T cells and CD8⁺ T cells responses induced by intramuscular injection of Ad5 vectored COVID-19 vaccine in phase I clinical study [54]. Nasal injection of an Ad5-expressing Ebola Zaire glycoprotein (Ad5-ZGP), which bypassed the influence of the pre-existing anti-Ad antibody, fully protected mice from a lethal challenge with Ebola [25]. The anti-Ad antibody did not influence either anti-RSV antibody induction by Ad-RSV-F *via* i.n. immunization or the induction of protection against RSV challenge in mice [6]. Indeed, pre-existing anti-Ad antibody did not influence the S-specific antibody responses which induced by AdCoV2 vaccine *via* i.n. or s.c. immunization (Fig. 9). Thus, the regiment for multiple injections of different Ad vaccines could be achieved to control SAS-CoV-2 variants or other infections in the future.

There were clinical observations of COVID-19 patients who had severe inflammatory responses in the lungs corresponding to viral burdens in the pulmonary epithelial cells and resulting in respiratory failure [55]. This finding also correlated with our result that pulmonary inflammation was recapitulated by Ad-LacZ immunization following a challenge with SARS-CoV-2 in animals. No or very mild inflammation in the lungs of mice that received AdCoV2-S was observed (Fig. 8). This consequence is corresponding to the Th1 cytokine and no proinflammatroy cytokine secretions except IFN-γ in the lungs of mice which received AdCoV2-S i.n. (Fig. 6).

Collectively, this evidence indicates that the protective immunogenicity of AdCoV2 is potent against SARS-CoV-2 infections. AdCoV2 administered through different routes of injection might induce different immune characteristics; mucosal *vs.* systemic immune responses, all showed that they can induce protective immune responses against SARS-CoV-2, while mucosal delivery of vaccine elicits the prevention of virus-induced lung inflammation and no vaccine-enhanced disease effects and prompts us to conduct further human trials.

Author contribution

Declaration of Competing Interest

Appendix A. Supplementary material

Supplementary data to this article can be found online at https://doi.org/10.1016/j.vaccine.2021.12.024.

References

[1] Ludwig Stephan, Zarbock SLAA. Coronaviruses and SARS-CoV-2: A Brief Overview. Anesthes Analgesi 2020;131(1):93–6.
[2] Walls AC, Park YJ, Tortorici MA, Wall A, McGuire AT, Veesler D. Structure, Function, and Antigenicity of the SARS-CoV-2 Spike Glycoprotein. Cell 2020;180:281–92.
[3] Robert N, Kirchdoerfer CAC, Wang N, Pallesen J, Yassine HM, Turner HL, et al. Pre-fusion structure of a human coronavirus spike protein. Nature 2016;531:118–21.
[4] Li F. Structure, Function, and Evolution of Coronavirus Spike Proteins. Ann Rev Virol 2016;3:237–61.
[5] Davidson AM, Wysocki J, Batlle D. Interaction of SARS-CoV-2 and Other Coronavirus With ACE (Angiotensin-Converting Enzyme)-2 as Their Main Receptor: Therapeutic Implications. Hypertension 2020;76:1339–49.
[6] Shao HY, Yu SL, Sia C, Chen Y, Chitra E, Chen IH, et al. Immunogenic properties of RSV-B1 fusion (F) protein gene-encoding recombinant adenoviruses. Vaccine 2009;4(27(40)):5460–71.
[7] Kohlmann R, Schwannecke S, Tippler B, Ternette N, Temchura VV, Tenbusch M, et al. Protective efficacy and immunogenicity of an adenoviral vector vaccine encoding the codon-optimized F protein of respiratory syncytial virus. J Virol 2009;83:12601–10.
[8] Coughlan L, Mullarkey C, Gilbert S. Adenoviral vectors as novel vaccines for influenza. J Pharm Pharmacol 2015;67:382–99.
[9] Smith KM, Pottage L, Thomas ER, Leishman AJ, Doig TN, Xu D, et al. Th1 and Th2 CD4+ T cells provide help for B cell clonal expansion and antibody synthesis in a similar manner in vivo. J Immunol 2000;165:3136–44.
[10] Barouch DH, Nabel GJ. Adenovirus vector-based vaccines for human immunodeficiency virus type 1. Hum Gene Ther 2005;16:149–56.
[11] Mosmann TR, Cherwinski H, Bond MW, Giedlin MA, Coffman RL. Two types of murine helper T cell clone. I. Definition according to profiles of lymphokine activities and secreted proteins. J Immunol 1986;136:2348–57.
[12] O'Garra A, Murphy K. Role of cytokines in determining T-lymphocyte function. Curr Opin Immunol 1994;6:458–66.
[13] Romagnani S. Lymphokine production by human T cells in disease states. Annu Rev Immunol 1994;12:227–57.
[14] Paul WE, Seder RA. Lymphocyte responses and cytokines. Cell 1994;76:241–51.
[15] Chaplin DD. Overview of the immune response. J Allergy Clin Immunol 2010;125:S3–S23.
[16] Tesmer LA, Lundy SK, Sarkar S, Fox DA. Th17 cells in human disease. Immunol Rev 2008;223:87–113.
[17] Crotty S. Follicular helper CD4 T cells (TFH). Annu Rev Immunol 2011;29:621–63.
[18] Ramiscal RR, Vinuesa CG. T-cell subsets in the germinal center. Immunol Rev 2013;252:146–55.
[19] Victora GD, Nussenzweig MC. Germinal centers. Annu Rev Immunol 2012;30:429–57.
[20] Li YD, Chi WY, Su JH, Ferrall L, Hung CF, Wu TC. Coronavirus vaccine development: from SARS and MERS to COVID-19. J Biomed Sci 2020;27:104.
[21] Wang J, Thorson L, Stokes RW, Santosuosso M, Huygen K, Zganiacz A, et al. Single mucosal, but not parenteral, immunization with recombinant adenoviral-based vaccine provides potent protection from pulmonary tuberculosis. J Immunol 2004;173:6357–65.
[22] Dong Y, Dai T, Wei Y, Zhang L, Zheng M, Zhou F. A systematic review of SARS-CoV-2 vaccine candidates. Sign Trans Target Ther 2020;5:237.
[23] Hassan AO, Kafai NM, Dmitriev IP, Fox JM, Smith BK, Harvey IB, et al. A Single-Dose Intranasal ChAd Vaccine Protects Upper and Lower Respiratory Tracts against SARS-CoV-2. Cell 2020;183(169–84):e13.
[24] Hassan AO, Feldmann F, Zhao H, Curiel DT, Okumura A, Tang-Huau TL, et al. A single intranasal dose of chimpanzee adenovirus-vectored vaccine protects against SARS-CoV-2 infection in rhesus macaques. Cell Rep Med 2021;2:100230.
[25] Croyle MA, Patel A, Tran KN, Gray M, Zhang Y, Strong JE, et al. Nasal delivery of an adenovirus-based vaccine bypasses pre-existing immunity to the vaccine carrier and improves the immune response in mice. PLoS ONE 2008;3:e3548.
[26] Shao HY, Yu SL, Sia C, Chen Y, Chitra E, Chen IH, et al. Immunogenic properties of RSV-B1 fusion (F) protein gene-encoding recombinant adenoviruses. Vaccine 2009;27:5460–71.
[27] Polack FP, Thomas SJ, Kitchin N, Absalon J, Gurtman A, Lockhart S, et al. Safety and Efficacy of the BNT162b2 mRNA Covid-19 Vaccine. New Engl J Med 2020;383:2603–15.
[28] Baden LR, El Sahly HM, Essink B, Kotloff K, Frey S, Novak R, et al. Efficacy and Safety of the mRNA-1273 SARS-CoV-2 Vaccine. New Engl J Med 2021;384:403–16.
[29] Brincks EL, Roberts AD, Cookenham T, Sell S, Kohlmeier JE, Blackman MA, et al. Antigen-specific memory regulatory CD4+Foxp3+ T cells control memory responses to influenza virus infection. J Immunol 2013;190:3438–46.
[30] Kossila M, Jauhiainen S, Laukkanen MO, Lehtolainen P, Jaaskelainen M, Turunen P, et al. Improvement in adenoviral gene transfer efficiency after preincubation at +37 degrees C in vitro and in vivo. Mol Ther 2002;5:87–93.
[31] Russell WC. Update on adenovirus and its vectors. J Gen Virol 2000;81:2573–604.
[32] Shao HY, Lin YW, Yu SL, Lin HY, Chitra E, Chang YC, et al. Immunoprotectivity of HLA-A2 CTL peptides derived from respiratory syncytial virus fusion protein in HLA-A2 transgenic mouse. PLoS ONE 2011;6:e25500.
[33] Holdsworth SR, Kitching AR, Tipping PG. Th1 and Th2 T helper cell subsets affect patterns of injury and outcomes in glomerulonephritis. Kidney Int 1999;55:1198–216.
[34] Gregory A, Poland IGO, Kennedy RB. SARS-CoV-2 immunity: review and applications to phase 3 vaccine candidates. Lancet 2020;396:1595–606.
[35] Imai M, Iwatsuki-Horimoto K, Hatta M, Loeber S, Halfmann PJ, Nakajima N, et al. Syrian hamsters as a small animal model for SARS-CoV-2 infection and countermeasure development. PNAS 2020;117:16587–95.
[36] Lee WS, Wheatley AK, Kent SJ, DeKosky BJ. Antibody-dependent enhancement and SARS-CoV-2 vaccines and therapies. Nat Microbiol 2020;5:1185–91.
[37] Graham BS. Vaccines against respiratory syncytial virus: The time has finally come. Vaccine 2016;34:3535–41.
[38] Nader PR, Warren RJ. Reported neurologic disorders following live measles vaccine. Pediatrics 1968;41:997–1001.
[39] Polack FP. Atypical measles and enhanced respiratory syncytial virus disease (ERD) made simple. Pediatr Res 2007;62:111–5.
[40] Honda-Okubo Y, Barnard D, Ong CH, Peng BH, Tseng CT, Petrovsky N. Severe acute respiratory syndrome-associated coronavirus vaccines formulated with delta inulin adjuvants provide enhanced protection while ameliorating lung eosinophilic immunopathology. J Virol 2015;89:2995–3007.
[41] Tseng CT, Sbrana E, Iwata-Yoshikawa N, Newman PC, Garron T, Atmar RL, et al. Immunization with SARS coronavirus vaccines leads to pulmonary immunopathology on challenge with the SARS virus. PLoS ONE 2012;7:e35421.
[42] Anywaine Z, Whitworth H, Kaleebu P, Praygod G, Shukarev G, Manno D, et al. Safety and Immunogenicity of a 2-Dose Heterologous Vaccination Regimen With Ad26.ZEBOV and MVA-BN-Filo Ebola Vaccines: 12-Month Data From a Phase 1 Randomized Clinical Trial in Uganda and Tanzania. J Infect Dis 2019;220:46–56.
[43] Baden LR, Karita E, Mutua G, Bekker LG, Gray G, Page-Shipp L, et al. Assessment of the Safety and Immunogenicity of 2 Novel Vaccine Platforms for HIV-1 Prevention: A Randomized Trial. Ann Intern Med 2016;164:313–22.
[44] Barouch DH, Tomaka FL, Wegmann F, Stieh DJ, Alter G, Robb ML, et al. Evaluation of a mosaic HIV-1 vaccine in a multicentre, randomised, double-blind, placebo-controlled, phase 1/2a clinical trial (APPROACH) and in rhesus monkeys (NHP 13–19). Lancet 2018;392:232–43.
[45] Shukarev G, Callendret B, Luhn K, Douoguih M, Consortium E. A two-dose heterologous prime-boost vaccine regimen eliciting sustained immune responses to Ebola Zaire could support a preventive strategy for future outbreaks. Human Vacc Immunother 2017;13:266–70.
[46] Rice A, Verma M, Shin A, Zakin L, Sieling P, Tanaka S, et al. Intranasal plus subcutaneous prime vaccination with a dual antigen COVID-19 vaccine elicits T-cell and antibody responses in mice. Sci Rep 2021;11:14917.
[47] Feng L, Wang Q, Shan C, Yang C, Feng Y, Wu J, et al. An adenovirus-vectored COVID-19 vaccine confers protection from SARS-COV-2 challenge in rhesus macaques. Nat Commun 2020;11:4207.
[48] Kim E, Weisel FJ, Balmert SC, Khan MS, Huang S, Erdos G, et al. A single subcutaneous or intranasal immunization with adenovirus-based SARS-CoV-2 vaccine induces robust humoral and cellular immune responses in mice. Eur J Immunol 2021;51:1774–84.
[49] King RG, Silva-Sanchez A, Peel JN, Botta D, Dickson AM, Pinto AK, et al. Single-Dose Intranasal Administration of AdCOVID Elicits Systemic and Mucosal Immunity against SARS-CoV-2 and Fully Protects Mice from Lethal Challenge. Vaccines 2021;9.
[50] Sterlin D, Mathian A, Miyara M, Mohr A, Anna F, Claer L, et al. IgA dominates the early neutralizing antibody response to SARS-CoV-2. Sci Transl Med 2021;13.

[51] Van Kampen KR, Shi Z, Gao P, Zhang J, Foster KW, Chen DT, et al. Safety and immunogenicity of adenovirus-vectored nasal and epicutaneous influenza vaccines in humans. Vaccine 2005;23:1029–36.

[52] Gallichan WS, Rosenthal KL. Long-term immunity and protection against herpes simplex virus type 2 in the murine female genital tract after mucosal but not systemic immunization. J Infect Dis 1998;177:1155–61.

[53] Shao HY, Hsu HS, Yu SL, Wu SR, Hu KC, Chang CK, et al. Immunogenicity of an adeno-vector vaccine expressing the F protein of a respiratory syncytial virus manufactured from serum-free suspension culture. Antiviral Res 2016;130:27–35.

[54] Zhu FC, Li YH, Guan XH, Hou LH, Wang WJ, Li JX, et al. Safety, tolerability, and immunogenicity of a recombinant adenovirus type-5 vectored COVID-19 vaccine: a dose-escalation, open-label, non-randomised, first-in-human trial. Lancet 2020;395:1845–54.

[55] Schaefer IM, Padera RF, Solomon IH, Kanjilal S, Hammer MM, Hornick JL, et al. In situ detection of SARS-CoV-2 in lungs and airways of patients with COVID-19. Mod Pathol Off J US Can Acad Pathol Inc 2020;33:2104–14.